doi.org/10.1007/978-3-642-80299-7_8

*Die Photochemischen Bildung des Chlorwasserstoffs*

# Dynamics of Cl + $H_2$ ⇌ HCl + H on a New Potential Energy Surface: The Photosynthesis of Hydrogen Chloride Revisited 100 Years after Max Bodenstein

Thomas C. Allison,[a] Steven L. Mielke,[a] David W. Schwenke,[b] Gillian C. Lynch,[a] Mark S. Gordon,[c] and Donald G. Truhlar[a]

[a]*Department of Chemistry, Chemical Physics Program, and Supercomputer Institute, University of Minnesota, 207 Pleasant Street SE, Minneapolis, MN 55455-0431, U.S.A.*

[b]*NASA Ames Research Center, Mail Stop 230-3, Moffett Field, CA 94035-1000, U.S.A.*

[c]*Department of Chemistry, Iowa State University, Ames, IA 50011, U.S.A.*

T. C. Allison, S. L. Mielke, D. W. Schwenke, G. C. Lynch, M. S. Gordon, and D. G. Truhlar, in *Gas-Phase Chemical Reaction Systems: Experiments and Models 100 Years after Max Bodenstein*, edited by J. Wolfrum, H.-R. Volpp, R. Rannacher, and J. Warnatz (Springer Series in Chemical Physics, Berlin, 1996), pp. 111-124.

***Abstract.*** In this contribution, we present a preliminary account of our recent work on the Cl + $H_2$ and Cl + $D_2$ reactions, which includes a new potential energy surface, variational transition state theory and semiclassical tunneling calculations for both reactions and for other isotopomeric cases, and accurate quantum dynamical calculations of rate constants and state-to-state integral and differential cross sections.

## 1. Introduction

Halogen atom–hydrogen molecule reactions and their reverse hydrogen atom–hydrogen halide reactions have played a major role in the development of chemical kinetics. The work of Bodenstein and Lind [1] on the $H_2$–$Br_2$ reaction led to the development of the chain mechanism [2–4] for free radical reactions and ultimately, with the steady-state assumption, to a value for the rate constant of the Br + $H_2$ reaction [5–10]. The work of Bodenstein and Dux [11–13] on the $Cl_2$–$H_2$ reaction also led to a chain mechanism for that case, with Cl eventually established as the chain carrier [7,14]. The $BrH_2$ and $ClH_2$ triatomic systems were the subjects of historical papers [15–17] in the development of the London-Eyring-Polanyi-Sato (LEPS) semiempirical valence bond treatment [18] for potential energy surfaces of atom transfer reactions. The F + $H_2$ reaction also has a long history and has been labeled the "bellwether" elementary reaction for showing the power and limitations of the methods of chemical dynamics [19]. The I + $H_2$ reaction is highly endothermic and hence slow; like the other halogen-hydrogen reactions it has been the subject of considerable controversy [10,20].

The Cl + $H_2$ ⇌ HCl + H reaction has a particularly long and interesting history, including thermal and photochemical studies of the $H_2$ – $Cl_2$ system, molecular beam experiments, measurements of perhaps the largest number of kinetic isotope effects known for any system, and a host of theoretical treatments. We will mention only a few particularly relevant studies. Early experimental studies of this reaction were often initiated by photodissociation of $Cl_2$, and some of the papers are entitled "Photosynthesis of Hydrogen Chloride" (a translation of *die Photochemischen Bildung des Chlorwasserstoffs*). These experimental studies of the hydrogen-chlorine photochemical reaction were

complicated by the existence of an induction period. The induction period was discovered by Draper in 1843 and studied further in 1857 by Bunsen and Roscoe, who believed it to be inherent in the mechanism; however, it was later shown by van't Hoff to be an experimental artifact. In 1906, Burgess and Chapman furthered clarified the effect as due to impurities. Chapman and McMahon suggested $NCl_3$ as the culprit a few years later, and the mechanism was only completely established in 1934 [21]. Additional controversy, in this case started by Bodenstein and Dux [11] and Chapman and Underhill [22], concerned the inhibiting effect of hydrogen, and this was resolved in 1933 [23].

At the same time that the mechanistic issues were being sorted out a rough estimate of the rate constant emerged. Bodenstein [24], based on earlier work on chain reactions by himself and others, estimated the probability $P$ of the reaction $H + Cl_2$ to be of the order of magnitude of $10^{-2}$, that for $H + HCl$ to be of the order of $10^{-4}$, and the equilibrium constant for $Cl + H_2 \rightleftharpoons HCl + H$ to be of order unity (a more accurate modern value at 298 K is 0.047 [26]); and hence his estimates yielded $P(Cl + H_2)$ to be $\sim 10^{-4}$. With a room-T collision rate coefficient of $4 \times 10^{-10}$ $cm^3molecule^{-1}s^{-1}$, this yields $k = 4 \times 10^{-14}$ $cm^3molecule^{-1}s^{-1}$. In 1933, Ritchie and Norrish obtained additional experimental evidence for $P(Cl + H_2)/P(H + Cl_2) = 10^{-2}$ and repeated the estimate $P(Cl + H_2) = 10^{-4}$.

The first "direct" measurement of the rate was carried out by Rodebush and Klingenhoefer [27] in 1933. They produced Cl by an electrodeless discharge, passed Cl and $H_2$ through a flow tube, quenched the reaction, and took samples after about 5–10 minutes (kilosecond chemistry). They titrated the products with KOH and methyl orange indicator and obtained $k(Cl + H_2) = 1.5 \times 10^{-14}$ $cm^3molecule^{-1}s^{-1}$ at room temperature, a factor of 3 lower than Bodenstein's estimate. The best value available at present is $1.50 \times 10^{-14}$ $cm^3molecule^{-1}s^{-1}$ [28], which is (fortuitously, but amazingly) identical to the 1933 value! (At 273 K, the best modern value is about 30% higher than the 1933 value.)

In 1932, Semenoff suggested that the activation energy $E_a$ be estimated by equating the rate constant to the collision rate constant times a Boltzmann factor; he obtained $E_a$ = 5.5–6.6 kcal [29]. In 1933 Ritchie and Norrish [25] estimated $E_a$ more directly from experiment. Using previous work [30–32] on the temperature coefficient (i.e., the amount by which the reaction rate goes up for a 10 deg increase in T) of the overall $H_2 - Cl_2$ chain reaction, which they took as 1.14 (with a large uncertainty), they estimated $E_a \cong 2.3$ kcal. In contrast, by the less reasonable assumption that two-body recombination of Cl occurs via $Cl(^2P_{1/2}) + Cl(^2P_{3/2}) \rightarrow Cl_2 + h\nu$, they obtained $E_a$ = 3.6 kcal. However a more recent (1932) measurement [33] of the temperature coefficient in an oxygen-free mixture (that they did not use) gave 1.37, which yields $E_a$ = 5.8 – 6.0 kcal [6,10]. The direct measurement of Rodebush and Klingenhoefer in 1933 yields $E_a$ = 5.6 kcal (obtained by fitting their data to standard Arrhenius form rather than the collision theory form they used). The best modern value is $E_a$ = 4.4 kcal, which would correspond to a temperature coefficient of 1.27 at 298 K [28].

The first kinetic isotope effect (KIE) measurement was reported in 1934, and it yielded $k_{H_2}/k_{D_2} \approx 10$ at room T [34]. Bigeleisen *et al.* obtained the same result in 1959 [35], and Chiltz *et al.* obtained 9 in 1963. The most recent values are 9.1 [95] and 7.5 [28]. By 1973, kinetic isotope effects were available for quite a few isotopomeric versions of the reaction [34–38].

The reverse abstraction reactions H + HCl → $H_2$ + Cl, D + DCl → $D_2$ + Cl, H + DCl → HD + Cl, and D + HCl → HD + Cl as well as the exchange reactions, H + DCl ↔ HCl + D, which compete with the back reactions, have also been studied experimentally, with the early work being quite controversial (even contradictory), as summarized elsewhere [26,39–42]. Two issues are involved: (i) Does detailed balance hold, i.e., does the forward rate constant divided by the backward abstraction rate constant equal the equilibrium constant? Some evidence pointed to possible deviations as great as a factor of two or three, which would raise interesting questions regarding nonequilibrium internal state distributions [43,44] during reaction. (ii) What is the relative rate of exchange compared to abstraction in the forward reaction? Issue (i) was settled by Miller and Gordon [26], who measured the reaction in both directions, and found that detailed balance holds quite well, as usually assumed. The best results for issue (ii) are also due to Miller and Gordon [41]. They placed an upper limit of $2 \times 10^{-3}$ on $k_{exch}/k_{abs}$ for D + HCl at 325 K. This implies a barrier height greater than about 7 kcal for exchange, whereas the molecular beam and infrared fluorescence experiments of McDonald and Herschbach [45] and Wight *et al.* [46] yield an upper bound in the range 20–22 kcal.

In 1991, Barclay *et al.* [47] reported single-collision studies of the competitive pathways of the D + HCl reaction for collision energies 27 and 43 kcal. The ratio of exchange to abstraction cross sections, $\sigma_{exch}/\sigma_{abs}$, was found to be about 2–3 at these high energies.

Returning to the forward reaction, we note that, due primarily to its small probability and nearly thermoneutral character, detailed dynamical studies (i.e., state-sensitive results or cross sections rather than thermal rate constants) have become available only very recently, in the crossed molecular beam (CMB) experiments of Casavecchia and coworkers [48]. At a collision energy of 6.4 kcal, they found that the DCl produced in the Cl + $D_2$ reaction is mainly scattered more than 80° backwards from the incident *D* direction (in the center-of-mass frame) and that about 80% of the total available energy is disposed into relative translation of the products.

Theoretical work, as always, must begin with a potential energy surface. Early work on the potential energy surface was quantitatively and sometimes qualitatively unreliable and is reviewed elsewhere [18]. In 1973, Stern, Persky, and Klein [49] created three semiempirical potential energy surfaces of the extended-LEPS type for comparison to kinetic isotope effects on the Cl + $H_2$ reaction. Although realistic for Cl–H–H type geometries, these surfaces are not globally satisfactory because they are quite unrealistic for H–Cl–H type geometries. The first globally realistic potential energy surface was due to Baer and Last, whose surface has a barrier height of 8.1 kcal for Cl + $H_2$, 5.1 kcal for the reverse abstraction reaction, and 12.5 kcal for the exchange reaction [50]. Unfortunately this surface predicts somewhat inaccurate rate constants and KIEs [51]. A more successful surface, based in part on electronic structure calculations with scaled [52] electron correlation for H–Cl–H type geometries, was published in 1989 [53]. This surface, called GQQ, has a barrier height of 7.7 kcal for the forward reaction, 4.7 kcal for the reverse abstraction, and 18.1 kcal for the exchange reaction. Barclay *et al.* [47] concluded from trajectory studies that the GQQ surface is adequate for the abstraction reaction and for the exchange reaction at 27 kcal but not for the exchange reaction at 36 kcal and higher.

It was noted in the concluding remarks of the paper presenting the GQQ surface [53] that this surface could be improved by incorporating *ab initio* calculations on the Cl–H–H bend potential. A surface incorporating this improvement has now been created [54] and is called G3. The barrier heights on the G3 surface are 7.9 kcal for Cl + $H_2$ and 4.9 and 18.1 kcal for the H + HCl abstraction and exchange reactions.

Returning for a moment to the general theme of halogen-$H_2$ reactions, we note that the methods used to obtain the GQQ and G3 surfaces for $ClH_2$ have also been used to obtain the most accurate currently available surfaces for $FH_2$ [55] and $BrH_2$ [56].

Dynamics calculations on the $ClH_2$ reactions also have a long history. Early work was based on conventional transition state theory (TST), without tunneling or with one-dimensional tunneling [16,47,57]. Later work included trajectory calculations [45,58–64], reduced-dimensionality studies [65–67], variational transition state theory (VTST) with multidimensional tunneling (MT) [68,69] or optimized multidimensional tunneling (OMT) [51,53,54], and approximate quantum scattering calculations [70]. In 1991 and 1993, Launay and coworkers presented converged quantum scattering calculations for the Cl + $H_2$ reaction on the GQQ surface [71,72], and Takada *et al.* [73] calculated accurate quantal reaction probabilities. The present account summarizes some of our recent dynamics calculations based on the G3 surface.

## 2. G3 potential energy surface

*Ab initio* electronic structure calculations were carried out for 63 Cl–H–H geometries by Møller-Plesset 4th order perturbation theory (MP4) [74] using valence triple zeta basis sets on Cl [75] and H [76] augmented by a set of five *d* functions on Cl and a set of *p* functions on H. The correlation energies were scaled by the MP4-SAC method [77] with scale factor 1/0.82. The geometries consisted of 21 sets of nearest-neighbor bond distances, each with Cl–H–H bond angle equal to 180, 170, and 160 deg.

The GQQ surface was modified by making the H-Cl triplet interaction in the LEPS function be an explicit function of all three internuclear distances. This allowed us to fit the *ab initio* Cl–H–H bending potentials with an RMS error of 0.08 kcal, while retaining the general shape of the GQQ potential for H–Cl–H and collinear Cl–H–H geometries.

## 3. Rate constants for Cl + $H_2$

Quantum mechanical rate constants were calculated for the Cl + $H_2$ reaction in three steps. First, we calculated converged cumulative reaction probabilities [78–80] for total angular momenta $J$ = 0–6. The calculations were performed using the outgoing wave variational principle [81,82] and techniques presented elsewhere [83,84]. Second, we used the separable rotation approximation (SRA) [85,86] to generate from a single $J$ the cumulative reaction probability up to as high a $J$ as is required for convergence. Third, we integrated these cumulative reaction probabilities, weighted by a Boltzmann factor and the appropriate kinematical and electronic partition function factors, to obtain thermal reaction rates.

Before presenting the results we comment on the validation of the SRA and the accuracy attainable with accurate quantum dynamical calculations by considering recent results for the D + $H_2$ → HD + H reaction [85,86]. The SRA is a shortcut allowing us to generate quantum dynamical rate constants, fully summed over $J$, from calculations at only one or a few

low $J$. In our initial studies of the method [85,86], we found that it is much more accurate if it is based on $J \geq K_{conv}$ where $K_{conv}$ is the highest value of the vibrational angular momentum quantum number [87] of the transition state that makes a significant contribution to the reaction rate. We would expect $K_{conv} < 6$ for reactions like D + $H_2$ and Cl + $H_2$ at temperatures of interest here, and rate constants for D + $H_2$ calculated from either $J = 3$ or $J = 5$ agree with full calculations with an average absolute error of only 3% over the range 200–1000 K [85,86]. Furthermore, full rate calculations agree with experiment [88] with an average absolute deviation of only 8% over this range of T. For D + $H_2$ accurate *ab initio* kinetics agree so well with experiment because the potential energy surfaces [89,90] are apparently very accurate. For Cl + $H_2$, then, comparison to experiment provides a check on the potential energy surface.

Table 1 shows SRA results for Cl + $H_2$ based on $J = 3$ and $J = 5$, and for this reaction the two sets of calculations agree with an average absolute deviation of only 1% over the 200–1000 K range. In contrast the average absolute deviation of the SRA results based on $J = 0$ (not shown) from those based on $J = 3$ or $J = 5$ is 23%.

Table 1 also shows a comparison to the values recommended [28] in the most recent evaluation of experimental data. On average the experimental rate constants are 42% lower than the quantal ones; the deviation could be accounted for by the barrier being too thin and the barrier height being about a half kcal (or more) too low on the G3 surface.

Table 1 also shows VTST/OMT results, in particular calculations carried out by improved canonical variational theory [91] with tunneling contributions included by the least-action ground-state approximation [92]. Anharmonicity is included by the WKB method [93] for stretches and by a semiclassical centrifugal oscillator method [94,95] for the bend. The average absolute deviation of the VTST/OMT calculations from the quantum scattering calculations is only 10%. This excellent agreement for the most quantum mechanical of the isotopes validates the use of the very inexpensive VTST/OMT method. Thus it is meaningful to use the VTST/OMT method for calculating KIEs.

Table 2 compares the present results to experiment for the KIEs. In this table, AB denotes Cl + AB → ACl + B, and BA denotes Cl + BA → BCl + A. Three sets of experimental data are shown: the collection of results from Stern, Persky, and Klein [49] and two sets of $k_{H_2}/k_{D_2}$ ratios: the results of Miller and Gordon [96] and the recommendation of Michael and coworkers [28]. The present results are given in the VTST/OMT column, followed by two sets of calculations based on conventional TST without tunneling. All the calculated results are based on the G3 surface; two of the calculations include anharmonicity as described above, and the final column shows conventional TST with no tunneling and harmonic partition functions, just to provide an old-fashioned point of reference. First of all we see that anharmonicity tends to decrease the predicted KIEs while more accurate inclusion of dynamics tends to increase them. The overall conclusion is that the present results may overestimate the tunneling, especially if we accept the most recent experimental results. This may be caused by the barrier being too thin, which is quite possibly a remnant of using the LEPS form as part of the fitting function, since the LEPS form seems to give barriers that are too thin, as discussed elsewhere [97].

The HD/DH results in Table 2 are especially worth emphasizing since this KIE is a very sensitive test of potential energy surfaces. In a

previous survey [51] of eleven potential energy surfaces the calculated values for $k_{HD}/k_{DH}$ at 300 K were, in chronological order of the development of the surfaces, 0.2, 0.2, 2.2, 1.8, 3.6, 2.6, 3.0, 0.3, 4.4, 3.1, and 1.9. Only three of these are within 40% of the experimental 1.8. Thus attaining a value within 40% of experiment can serve as a criterion of good quality.

Figure 1 shows the quantum scattering theory calculations of the cumulative reaction probability (CRP), $N^0(E)$, for Cl + para $H_2$ for total angular momentum zero. The CRP is the sum of all state-to-state reaction probabilities at a given total energy [78–80], and it is directly related to the rate constant $k^0(E)$ for a microcanonical ensemble with zero total angular momentum at the total energy $E$. In particular

$$k^0(E) = [h\rho^R(E)]^{-1}N^0(E) \qquad (1)$$

where $h$ is Planck's constant, and $\rho^R(E)$ is the reactant density of states, which carries no dynamical information. One advantage of modern quantum scattering theory as compared to experiment is that we can look at $k^0(E)$ and $N^0(E)$ which are impractical to *measure* for bimolecular reactions. The advantage of being able to do this is that $N^0(E)$ is more directly related to the structure and dynamical properties of the transition state than is the usual canonical-ensemble rate constant $k(T)$. In fact the step structure faintly observable in Fig. 1 is a direct consequence of the quantized nature of the transition state [80,98,99]. This structure is brought out more clearly in the derivative curve $\rho^0(E) = dN^0/dE$; $\rho^0(E)$ is called the density of reactive states [80,98,99] and may be considered to represent the Holy Grail of chemistry—the spectrum of the transition state. The density of reactive states for Cl + para $H_2$ is shown in Fig. 2, and it shows several quantized states clearly. The assignment of these states is most easily made by studying the vibrationally adiabatic potential energy curves defined by [91]:

$$V_a(v_1,v_2,K,s) = V_{MEP}(s) + \varepsilon(v_1,v_2,K,s) \qquad (2)$$

where $V_{MEP}(s)$ is the Born-Oppenheimer potential energy along the minimum energy path (MEP) as a function of the reaction coordinate $s$, $\varepsilon(v_1,v_2,s)$ are the vibrational energies of the generalized transition states, $v_1$ is the stretching quantum number for the mode that adiabatically transforms from an H-H stretch to a quasisymmetric stretch of the Cl-H-H transition state to an H-Cl stretch, and $v_2$ is the bending quantum number of the transition state. As usual [87], the quantum numbers are displayed as $v_1v_2^K$. The relation of the adiabatic energies to transition state theory has a long history, dating back to Hirschfelder and Wigner [100], and it was eventually clarified in 1979 by the proof that the adiabatic theory of reactions [101] is identical to microcanonical variational transition state theory [102]. Thus the maxima of the vibrationally adiabatic curves are identified with dynamical bottlenecks.

The density of reactive states was fit to a sum of contributions with line shapes [80,98] corresponding to parabolic effective barriers. The individual terms in the fit are shown in Fig. 2, and the area under each term corresponds to the transmission coefficient for an individual quantized level of the transition state [80,98]. To interpret the fit, we calculated the vibrationally adiabatic curves and scaled the vibrational energies so that the energies of the maxima agree with the energy levels obtained from the fits; these curves are shown in Fig. 3. The interpretation of the CRP is now very clear: The reaction threshold at 11 kcal corresponds to the ground state of the transition state (TS), which is a nearly ideal bottleneck since $\kappa \approx 1$. (The tail extending to lower energy is due to

tunneling as are the low-energy sides of *all* the peaks.) At 15.3 kcal, the first excited state of the TS is accessed, which allows more flux to pass. However, although motion is locally vibrationally adiabatic near the TS, the curvature of the reaction path causes some transitions to $v_1 = 1$, and reflection occurs when the systems hits the local maximum in $V_a(1,0,0,s)$ at $s \approx 0.6\ a_0$. At 17.4 kcal, this local bottleneck is surmounted, and the reflection mechanism closes down, but the CRP can only rise to $\lesssim 2$ because the state count of 2 at the variational transition state near $s = 0$ is still globally limiting the flux. At about 19.6 kcal one encounters both the $04^0$ state and the global maximum of the $10^0$ curve. The latter is the $10^0$ variational transition state, and the lower-energy $10^0$ feature is a supernumerary transition state of the first kind, in the classification presented elsewhere [103]. The lifetimes of the dynamical bottlenecks in a quantum mechanical world (calculated from their widths in the energy domain) are consistent with the shapes of the vibrationally adiabatic curves: 14, 9, and 7 fs for peaks 1, 2, and 4, respectively, as the bending excitation makes the effective barriers thinner, and 26–29 fs for peaks 3 and 5 associated with broader barriers.

## 4. Cross sections

Another valuable use of accurate quantum dynamics calculations is testing the validity of classical simulations for predicting product-state distributions, and reduced-dimensionality studies of this issue are available for both Cl + $H_2$ [67] and H + $Cl_2$ [104]. In the present case extensive quasiclassical trajectory (QCT) calculations have been carried out for the full-dimensional Cl + $D_2$ reaction by Aoiz and Banares [105]. An example of how the QCT results compare to the accurate quantum ones is given in Fig. 4, which shows differential cross sections for Cl + $D_2(v=0,j=1)$ $\rightarrow$ DCl($v'$) + D, where $v$ and $v'$ are initial and final vibrational quantum number, respectively, $j$ is initial rotational quantum number, and the results are summed over final rotational quantum number $j'$. The comparison in Fig. 4 is for an initial relative translational energy of 10.1 kcal. The agreement is quite good. Notice, however, that the QCT method overestimates the amount of vibrationally excited product.

Finally, we also note that *preliminary* comparison to Cl + $H_2$ molecular beam results [48] at low energy (6 kcal) shows good agreement for both angular and time-of-flight distributions of the products [106].

## 5. Acknowledgments

The assistance of Joan Gordon is gratefully acknowledged. The quantum scattering calculations were supported in part by the National Science Foundation under grant no. CHE94-23927, the VTST work was supported in part by the U.S. Department of Energy, Office of Basic Energy Sciences under grant no. FG02-86ER13579 and the electronic structure calculations were supported in part by a grant from the Air Force Office of Scientific Research (F49620-95-1-0077).

## References

[1] M. Bodenstein and S. C. Lind: Z. Phys. Chem. (Leipzig) **57**, 168 (1906).

[2] J. A. Christiansen: K. Dan. Vidensk. Selsk. Mat. Phys. Medd. 1, 14 (1919).

[3] K. F. Herzfeld: Ann. Phys. (Leipzig) **59**, 635 (1919).

[4] M. Polanyi: Z. Elektrochem. **26**, 50 (1920).
[5] L. S. Kassel: *The Kinetics of Homogeneous Gas Reactions* (Chemical Catalog Co., New York, 1932), pp. 237–248, 267–276.
[6] N. Semenoff: *Chemical Kinetics and Chain Reactions* (Oxford University Press, London, 1935), pp. 89–122, 140–153.
[7] K. J. Laidler: *Chemical Kinetics*, 3rd ed. (Harper & Row, New York, 1987), pp. 14, 288–298.
[8] J. W. Moore and R. G. Pearson: *Kinetics and Mechanism*, 3rd ed. (John Wiley & Sons, New York, 1981), pp. 3, 390–394.
[9] G. G. Hammes: *Principles of Chemical Kinetics* (Academic, New York, 1978), pp. 76–79.
[10] G. C. Fettis and J. H. Knox: Prog. Reaction Kinetic. 2, 1 (1964).
[11] M. Bodenstein and W. Dux: Z. Phys. Chem. (Leipzig) **85**, 297 (1913).
[12] M. Bodenstein: Z. Elektrochem. **85**, 329 (1913).
[13] M. Bodenstein: Z. Elektrochem. **22**, 52 (1916).
[14] W. Nernst: Z. Elektrochem. **24**, 335 (1918).
[15] H. Eyring and M. Polanyi: Z. Phys. Chem. (Leipzig) **B12**, 279 (1931).
[16] A. Wheeler, B. Topley, and H. Eyring: J. Chem. Phys. 4, 178 (1936).
[17] S. Sato: J. Chem. Phys. **23**, 2465 (1955).
[18] C. A. Parr and D. G. Truhlar: J. Phys. Chem. **75**, 1844 (1971).
[19] R. D. Levine and R. B. Bernstein: *Molecular Reaction Dynamics and Chemical Reactivity* (Oxford University Press, New York, 1987), pp. 396–411.
[20] J. H. Sullivan: J. Chem. Phys. **30**, 1292 (1959).
[21] J. G. A. Griffiths and R. G. W. Norrish: Proc. Roy. Soc. Lond., Ser. A **147**, 140 (1934).
[22] D. L. Chapman and L. K. Underhill: J. Chem. Soc. **103**, 496 (1913).
[23] R. G. W. Norrish and M. Ritchie: Proc. Roy. Soc. Lond. Ser. A **140**, 713 (1933).
[24] M. Bodenstein: Trans. Faraday Soc. **27**, 413, 427 (1931).
[25] M. Ritchie and R. G. W. Norrish: Proc. Roy. Soc. Lond. Ser. A **140**, 112 (1933).
[26] J. C. Miller and R. J. Gordon: J. Chem. Phys. **75**, 5305 (1981).
[27] W. H. Rodebush and W. C. Klingenhoefer: J. Amer. Chem. Soc. **55**, 130 (1933).
[28] S. S. Kumaran, K. P. Lim, and J. V. Michael: J. Chem. Phys. **101**, 9487 (1994).
[29] N. Semenoff: Phys. Z. d. Sowjetunion **1**, 718 (1932).
[30] Padoa and Buttironi: Gazz. Chim. Ital. (II) **47**, 6 (1917).
[31] F. Porter, D. C. Bardwell, and S. C. Lind: J. Amer. Chem. Soc. **48**, 2603 (1926).
[32] S. C. Lind and R. Livingston: J. Amer. Chem. Soc. **52**, 593 (1930).
[33] E. Hertel: Z. Phys. Chem. (Leipzig) B **15**, 325 (1932).
[34] G. K. Rollefson: J. Chem. Phys. **2**, 144 (1934).
[35] J. Bigeleisen, F. S. Klein, R. E. Weston, Jr., and M. Wolfsberg: J. Chem. Phys. **30**, 1340 (1959).
[36] G. Chiltz, R. Eckling, P. Goldfinger, G. Huybrechts, H. S. Johnson, L. Meyers, and G. Verbeke: J. Chem. Phys. **38**, 1053 (1963).
[37] A. Persky and F. S. Klein: J. Chem. Phys. **44**, 3617 (1966).
[38] Y. Bar Yaakov, A. Persky, and F. S. Klein: J. Chem. Phys. **59**, 2415 (1973).
[39] F. S. Klein and I. Veltman: J. Chem. Soc. Faraday Trans. II **74**, 17 (1978).
[40] R. E. Weston, Jr.: J. Phys. Chem. **83**, 61 (1979).

[41] J. C. Miller and R. J. Gordon: J. Chem. Phys. **78**, 3713 (1983).
[42] D. G. Truhlar, F. B. Brown, D. W. Schwenke, R. Steckler, and B. C. Garrett: in *Comparison of Ab Initio Quantum Chemistry with Experiment for Small Molecules*, edited by R. J. Bartlett (Reidel, Dordrecht, 1985), p. 95.
[43] R. K. Boyd: Chem. Rev. **77**, 93 (1977).
[44] C. Lim and D. G. Truhlar: J. Chem. Phys. **79**, 3296 (1983).
[45] J. D. McDonald and D. R. Herschbach: J. Chem. Phys. **62**, 4740 (1975).
[45] C. A. Wight, F. Magnotta, and S. R. Leone: J. Chem. Phys. **81**, 3951 (1984).
[47] V. J. Barclay, B. A. Collings, J. C. Polanyi, and J. H. Wang: J. Phys. Chem. **95**, 2921 (1991).
[48] M. Alagia, N. Bulacani, P. Casavecchia, D. Stranges, and G. G. Volpi: J. Chem. Soc. Faraday Trans. **91**, 575 (1995).
[49] M. J. Stern, A. Persky, and F. S. Klein: J. Chem. Phys. **58**, 5697 (1973).
[50] M. Baer and I. Last: in P*otential Energy Surfaces and Dynamics Calculations*, edited by D. G. Truhlar (Plenum, New York, 1981), p. 519.
[51] S. C. Tucker, D. G. Truhlar, B. C. Garrett, and A. D. Isaacson: J. Chem. Phys. **82**, 4102 (1985).
[52] F. B. Brown and D. G. Truhlar: Chem. Phys. Lett. **117**, 307 (1985).
[53] D. W. Schwenke, S. C. Tucker, R. Steckler, F. B. Brown, G. C. Lynch, and D. G. Truhlar, J. Chem. Phys. **90**, 3110 (1989).
[54] T. C. Allison, S. L. Mielke, G. C. Lynch, D. G. Truhlar, and M. S. Gordon, to be published.
[55] S. L. Mielke, G. C. Lynch, D. G. Truhlar, and D. W. Schwenke: Chem. Phys. Lett. **213**, 10 (1993), **217**, 173(E) (1994).
[56] G. C. Lynch, D. G. Truhlar, F. B. Brown, and J.-g. Zhao: J. Phys. Chem. **99**, 207 (1995).
[57] M. Salomon: Int. J. Chem. Kinet. **2**, 175 (1984).
[58] D. L. Thompson, H. H. Suzukawa, Jr., and L. M. Raff: J. Chem. Phys. **62**, 4727 (1975).
[59] A. Persky: J. Chem. Phys. **66**, 2932 (1977)
[60] A. Persky: J. Chem. Phys. **68**, 2411 (1978).
[61] A. Persky: J. Chem. Phys. **70**, 3910 (1979).
[62] T. Valencich, J. Hsieh, J. Kwan, T. Stewart, and T. Lenhardt: Ber. Bunsenges. Phys. Chem. **81**, 131 (1977).
[63] A. Persky and M. Broida: J. Chem. Phys. **84**, 2653 (1986).
[64] P. M. Aker and J. J. Valentini: Isr. J. Chem. **30**, 157 (1990).
[65] M. Baer: Mol. Phys. **27**, 1429 (1974).
[66] A. Persky and M. Baer: J. Chem. Phys. **60**, 133 (1974).
[67] M. Baer, U. Halavee, and A. Persky: J. Chem. Phys. **61**, 5122 (1974).
[68] B. C. Garrett, D. G. Truhlar, and A. W. Magnuson: J. Chem. Phys. **74**, 1029 (1981).
[69] B. C. Garrett, D. G. Truhlar, and A. W. Magnuson: J. Chem. Phys. **76**, 2321 (1982).
[70] D. C. Clary: Chem. Phys. Lett. **80**, 271 (1981).
[71] J. M. Launay and S. B. Padkjær: Chem. Phys. Lett. **181**, 95 (1991).
[72] S. E. Branchett, S. B. Padkjær, and J. M. Launay: Chem. Phys. Lett. **208**, 523 (1993).
[73] S. Takada, K. Tsuda, A. Ohsaki, and H. Nakamura: Adv. Mol. Vib. Coll. Dyn. **2A**, 245 (1994).

[74] W. J. Hehre, L. Radom, P.v.R. Schleyer, and J. A. Pople: *Ab Initio Molecular Orbital Theory* (John Wiley & Sons, New York, 1986), pp. 38–40.
[75] A. D. McLean and G. S. Chandler: J. Chem. Phys. **72**, 5639 (1980).
[76] M. J. Frisch, J. A. Pople, and J. S. Binkley: J. Chem. Phys. **80**, 3265 (1984).
[77] M. S. Gordon and D. G. Truhlar: J. Amer. Chem. Soc. **108**, 5412 (1986).
[78] D. C. Chatfield, D. G. Truhlar, and D. W. Schwenke: J. Chem. Phys. **94**, 2040 (1991).
[79] W. H. Miller: J. Chem. Phys. **62**, 1899 (1975).
[80] D. C. Chatfield, R. S. Friedman, D. G. Truhlar, B. C. Garrett, and D. W. Schwenke: J. Amer. Chem. Soc. **113**, 486 (1991).
[81] Y. Sun, D. J. Kouri, D. G. Truhlar, and D. W. Schwenke: Phys. Rev. A **41**, 4857 (1990).
[82] Y. Sun, D. J. Kouri, and D. G. Truhlar: Nucl. Phys. **A508**, 41c (1990).
[83] D. W. Schwenke, S. L. Mielke, and D. G. Truhlar: Theor. Chim. Acta **79**, 241 (1991).
[84] G. J. Tawa, S. L. Mielke, D. G. Truhlar, and D. W. Schwenke: Adv. Mol. Vib. Coll. Dyn. **2B**, 45 (1994).
[85] S. L. Mielke, G. C. Lynch, D. G. Truhlar, and D. W. Schwenke: Chem. Physics Lett. **216**, 441 (1993).
[86] S. L. Mielke, G. C. Lynch, D. G. Truhlar, and D. W. Schwenke: J. Phys. Chem. **98**, 8000 (1994).
[87] G. Herzberg: Infrared and Raman Spectra Polyatomic of Polyatomic Molecules (van Nostrand, Princeton, 1945), pp. 210–211, 273–276.
[88] J. V. Michael and J. R. Fisher: J. Phys. Chem. 94, 3318 (1990).
[89] D. G. Truhlar and C. J. Horowitz: J. Chem. Phys. **68**, 2466 (1978), **71**, 1514(E) (1979).
[90] A. J. C. Varandas, F. B. Brown, C. A. Mead, D. G. Truhlar, and N. C. Blais: J. Chem. Phys. **86**, 6258 (1987).
[91] B. C. Garrett, D. G. Truhlar, R. S. Grev, and A. W. Magnuson: J. Phys. Chem. **84**, 1730 (1980).
[92] B. C. Garrett and D. G. Truhlar: J. Chem. Phys. **79**, 4931 (1983).
[93] B. C. Garrett and D. G. Truhlar: J. Chem. Phys. **81**, 309 (1984).
[94] G. A. Natanson: J. Chem. Phys. **93**, 6589 (1990).
[95] B. C. Garrett and D. G. Truhlar: J. Phys. Chem. **95**, 10374 (1991).
[96] J. C. Miller and R. J. Gordon: J. Chem. Phys. **79**, 1252 (1983).
[97] D. G. Truhlar and R. E. Wyatt: Adv. Chem. Phys. **36**, 141 (1977).
[98] D. C. Chatfield, R. S. Friedman, D. W. Schwenke, and D. G. Truhlar: J. Phys. Chem. **96**, 2414 (1992).
[99] D. C. Chatfield, R. S. Friedman, S. L. Mielke, D. W. Schwenke, G. C. Lynch, T. C. Allison, and D. G. Truhlar: in *Dynamics of Molecules and Chemical Reactions*, edited by R. E. Wyatt and J. Z. H. Zhang (Dekker, New York), in press.
[100] J. O. Hirschfelder and E. Wigner: J. Chem. Phys. **7**, 616 (1939).
[101] D. G. Truhlar: J. Chem. Phys. **53**, 2041 (1970).
[102] B. C. Garrett and D. G. Truhlar: J. Phys. Chem. **83**, 1079 (1979), **87** 4553(E) (1983).
[103] D. C. Chatfield, R. S. Friedman, G. C. Lynch, D. G. Truhlar, and D. W. Schwenke: J. Chem. Phys. **98**, 342 (1993).
[104] D. G. Truhlar, J. A. Merrick, and J. W. Duff: J. Chem. Phys. **98**, 6771 (1976).
[105] F. J. Aoiz and L. Banares: unpublished.
[106] P. Casavecchia: private communication.

Table 1. Rate constants ($cm^3molecule^{-1}s^{-1}$) for $Cl + H_2$

| | SRA | | | |
|---|---|---|---|---|
| T(K) | $J=3$ | $J=5$ | VTST/OMT | Experiment[28] |
| 200 | 8.49(–16) | 8.66(–16) | 8.96(–16) | 3.92(–16) |
| 300 | 2.48(–14) | 2.50(–14) | 2.31(–14) | 1.57(–14) |
| 400 | 1.50(–13) | 1.51(–13) | 1.31(–13) | 9.89(–14) |
| 600 | 1.00(–12) | 1.01(–12) | 8.68(–13) | 7.19(–13) |
| 800 | 2.79(–12) | 2.80(–12) | 2.52(–12) | 2.24(–12) |
| 1000 | 5.41(–12) | 5.46(–12) | 4.92(–12) | 4.85(–12) |

Table 2. Kinetic isotope effects $k_{AB}/k_{CD}$

| | | Experiment | | | VTST/OMT | TST | TST |
|---|---|---|---|---|---|---|---|
| AB/CD | T(K) | '73[49] | '83[95] | '94[28] | anhar | anhar | har |
| $H_2/D_2$ | 245 | 14.6 | | | 15.0 | 8.7 | 12.3 |
| | 255 | | 12.9 | 9.4 | 13.9 | 8.3 | 11.4 |
| | 298 | | 9.1 | 7.5 | 10.6 | 6.7 | 8.7 |
| | 345 | 7.5 | 6.9 | 6.1 | 8.3 | 5.6 | 7.0 |
| | 500 | | 4.0 | 3.6 | 4.9 | 3.8 | 4.3 |
| | 600 | | | 3.0 | 3.9 | 3.2 | 3.5 |
| | 1000 | | | 2.1 | 2.3 | 2.2 | 2.3 |
| $H_2/T_2$ | 275 | 34.2 | | | 50.7 | 20.4 | 30.0 |
| | 345 | 18.3 | | | 26.5 | 13.1 | 17.4 |
| HD/DH | 300 | 1.76 | | | 2.1 | 1.29 | 1.41 |
| | 445 | 1.37 | | | 1.79 | 1.25 | 1.31 |
| $H_2/(HD+DH)$ | 245 | 3.4 | | | 4.4 | 2.5 | 2.9 |
| | 345 | 2.5 | | | 3.1 | 2.1 | 2.3 |
| $H_2/(HT+TH)$ | 245 | 6.5 | | | 10.8 | 3.4 | 4.2 |
| | 345 | 4.1 | | | 6.0 | 2.7 | 3.2 |
| $H_2/(DT+TD)$ | 275 | 20.7 | | | 25.7 | 11.8 | 16.6 |
| | 345 | 12.1 | | | 15.3 | 8.3 | 10.7 |

**Figure captions**

Fig. 1. Accurate quantal cumulative reaction probability $N^0(E)$ for Cl + para $H_2 \rightarrow$ HCl + H on the G3 surface.

Fig. 2. Density of reactive states, $\rho^0(E)$, for Cl + para $H_2$ with $J = 0$ on the G3 surface. Heavy solid curve: accurate quantal; heavy dashed curve: fit; light dashed curve: components of the fit. The energies, state assignments, and transmission coefficients of the quantized transition state energy levels are indicated next to arrows at the energies of the peaks in the components of the fit.

Fig. 3. $V_{MEP}(s)$ and $V_a(v_1,v_2,K,s)$ for Cl + para $H_2 \rightarrow$ HCl + H on the G3 surface vs. reaction coordinate $s$.

Fig. 4. Differential cross section vs. scattering angle for Cl + $D_2(v=0,j=1) \rightarrow$ DCl($v'$) + D as a function of scattering angle. The results from quantum scattering theory are compared to those from quasiclassical trajectories for a collision energy of 10.1 kcal.

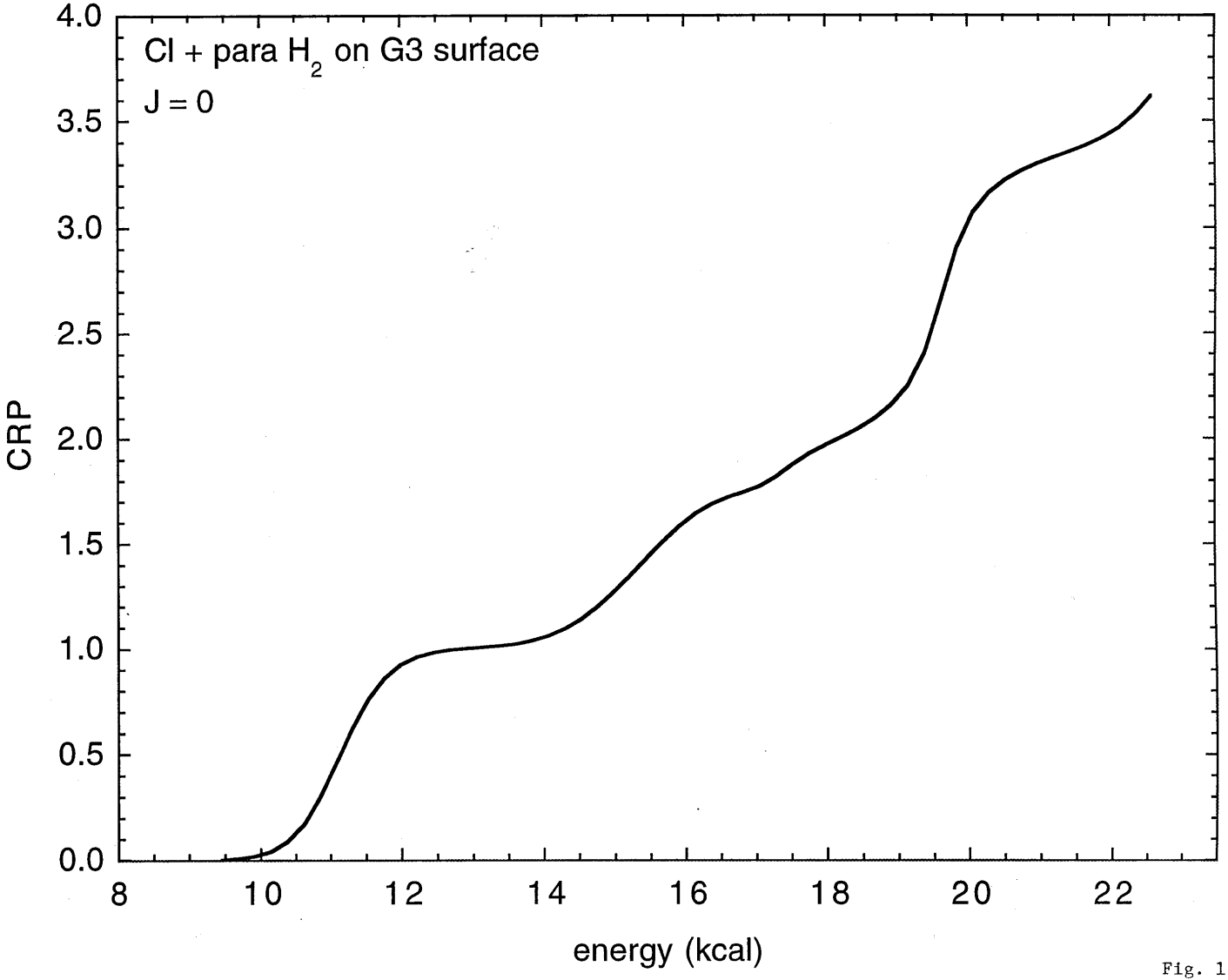
Cl + para $H_2$ on G3 surface
J = 0
CRP
energy (kcal)
4.0
3.5
3.0
2.5
2.0
1.5
1.0
0.5
0.0
8
10
12
14
16
18
20
22

Fig. 1

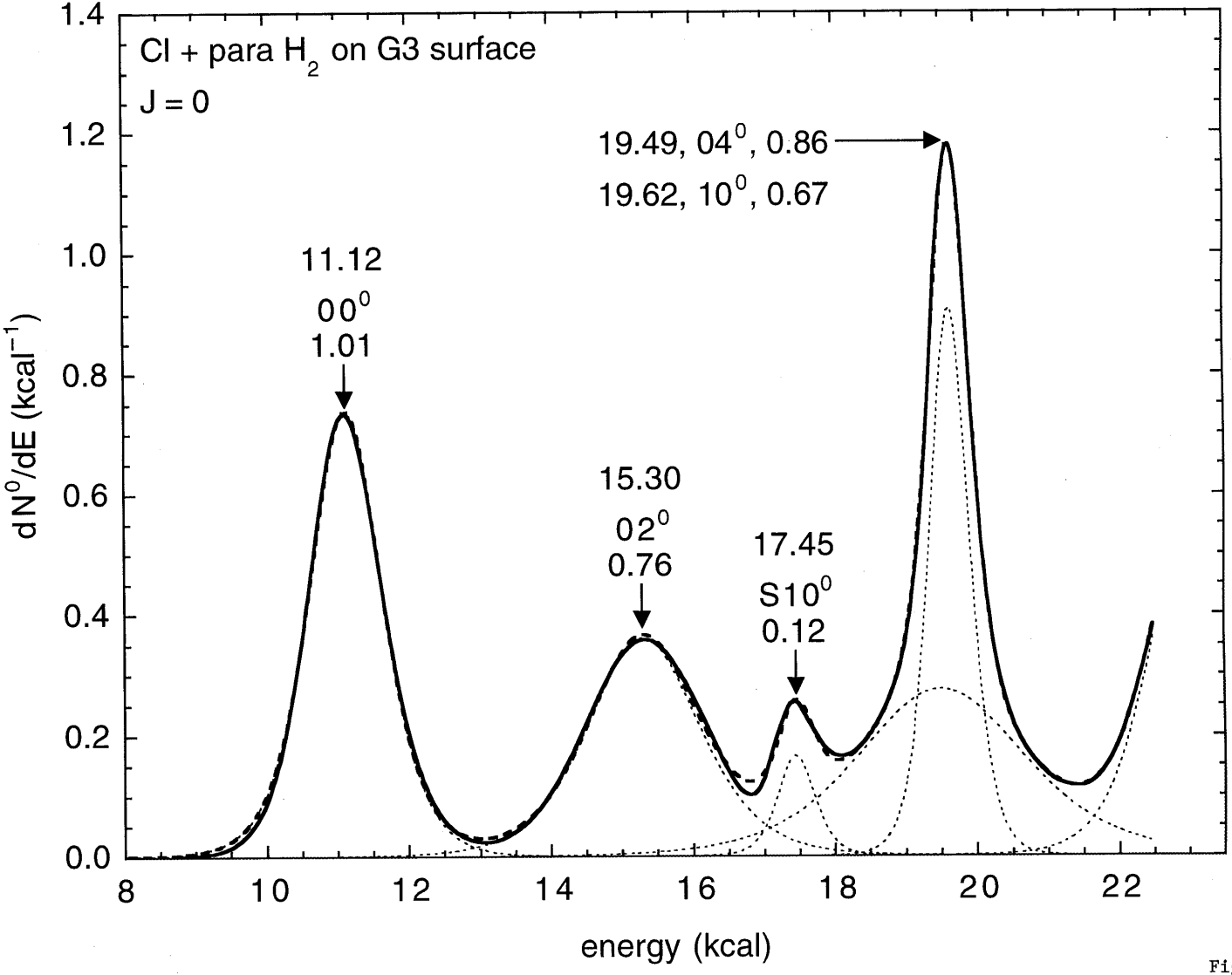
Cl + para $H_2$ on G3 surface
J = 0
19.49, $04^0$, 0.86
19.62, $10^0$, 0.67
11.12
$00^0$
1.01
15.30
$02^0$
0.76
17.45
$S10^0$
0.12
$dN^0/dE$ (kcal$^{-1}$)
energy (kcal)
0.0
0.2
0.4
0.6
0.8
1.0
1.2
1.4
8
10
12
14
16
18
20
22

Fig. 2

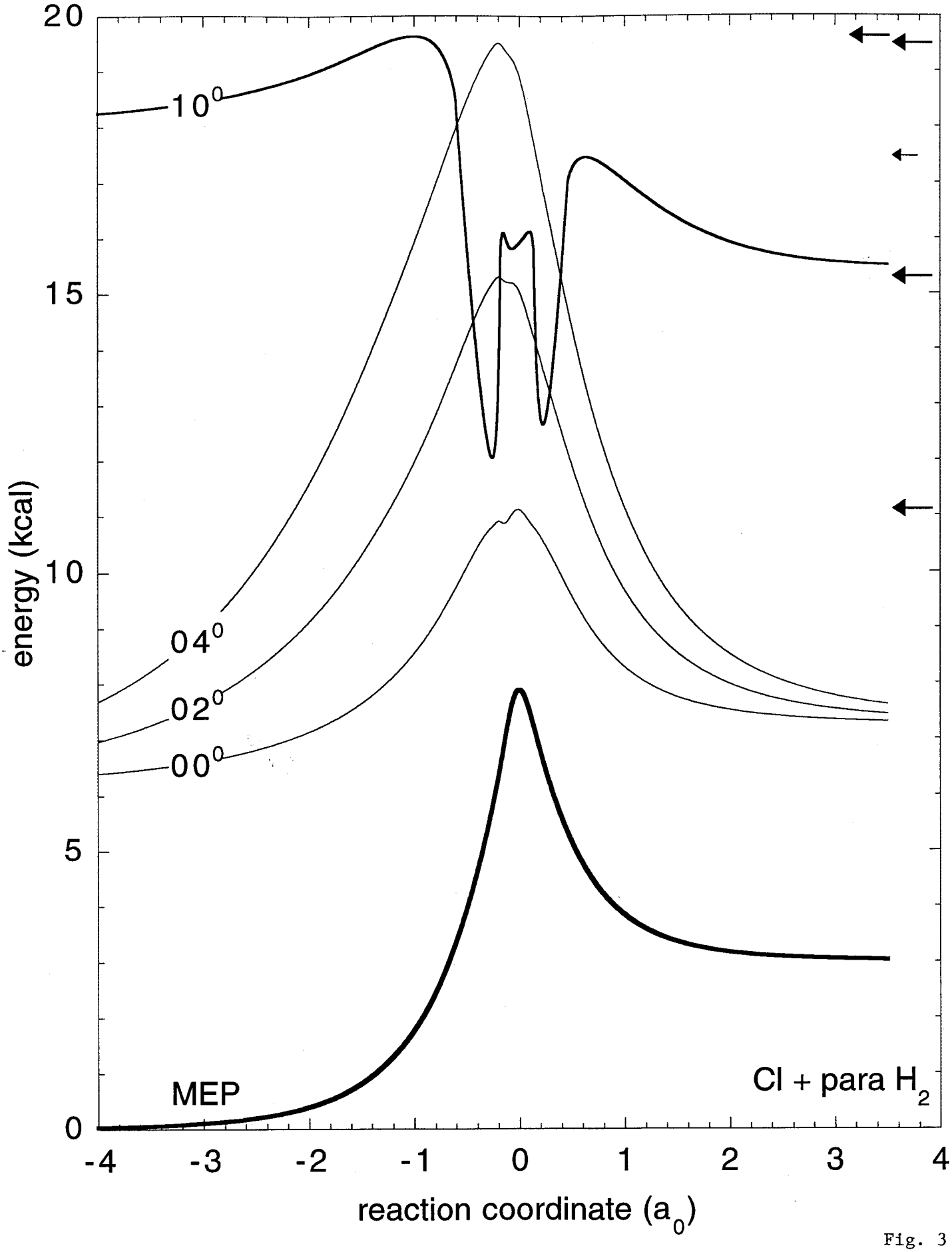
20
15
10
5
0
energy (kcal)
$10^0$
$04^0$
$02^0$
$00^0$
MEP
Cl + para $H_2$
-4
-3
-2
-1
0
1
2
3
4
reaction coordinate ($a_0$)

Fig. 3

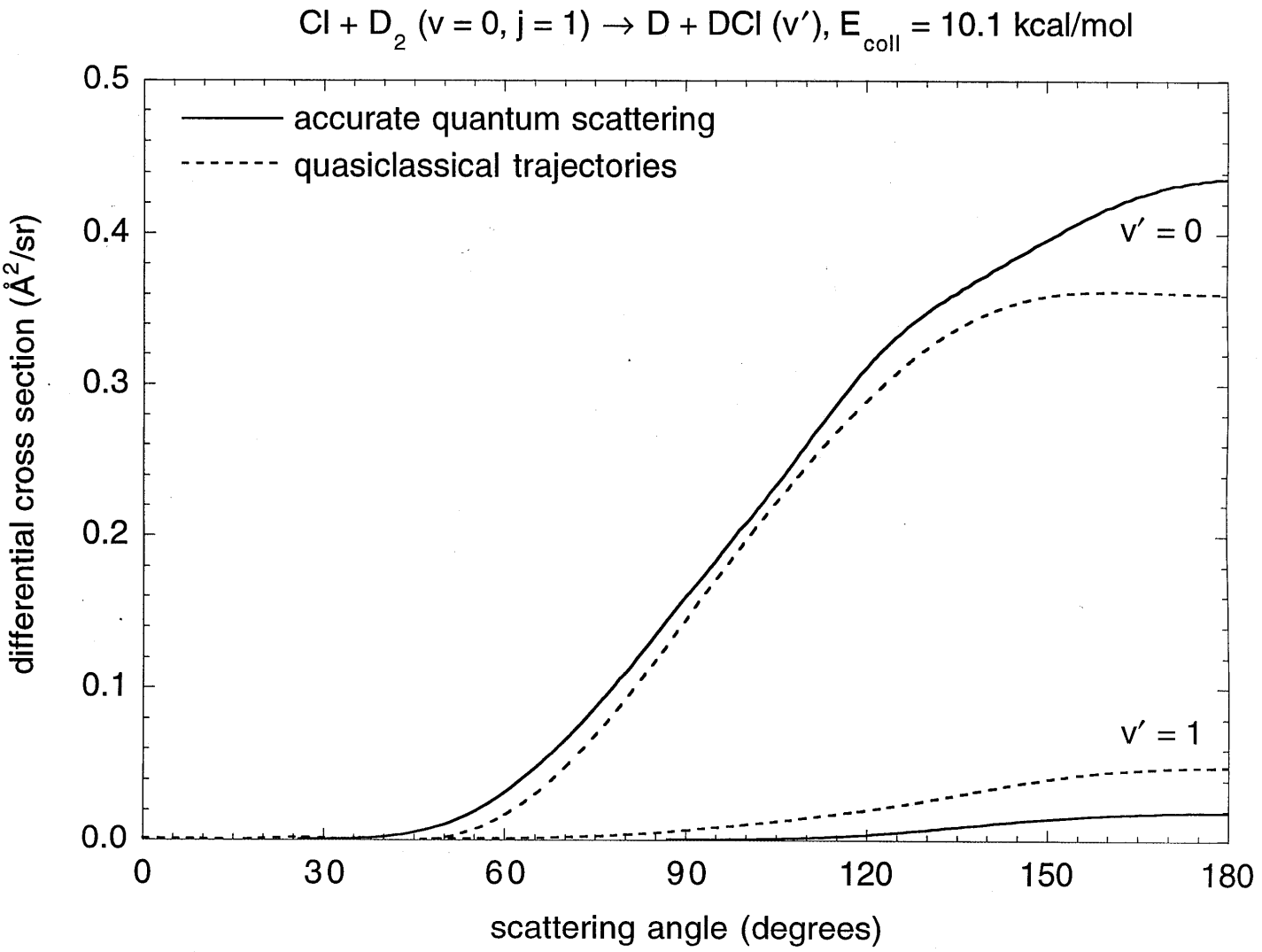
Cl + D2 (v = 0, j = 1) → D + DCl (v′), Ecoll = 10.1 kcal/mol
accurate quantum scattering
quasiclassical trajectories
v′ = 0
v′ = 1
differential cross section (Å2/sr)
0.0
0.1
0.2
0.3
0.4
0.5
0
30
60
90
120
150
180
scattering angle (degrees)

Fig. 4